Phase behavior, structural effects, and volumetric and transport properties in nonaqueous microemulsions

S. K. Mehta,* Kawaljit, and Kiran Bala

Department of Chemistry, Panjab University, Chandigarh 160014, India

(Received 24 August 1998)

We report here results concerning nonaqueous microemulsions containing sodium bis(2-ethylhexyl)sulfosuccinate (AOT)+hexane+nonaqueous polar component, i.e., ethyleneglycol/2-pyrrolidinone/glycerol/methanol, over a wide range of volume fraction (ϕ) of dispersed phase at 30 °C. The influence of such nonaqueous systems on conductivity, dynamic viscosity, density, and ultrasonic velocity have been investigated. Electrical conductivity (σ) and viscosity (η) data show the existence of a percolation threshold. An excellent agreement between the $(\sigma/\phi)_{expt}$ and $(\sigma/\phi)_{calc}$ calculated from the prediction of the droplet charge fluctuation model has been observed. The aggregation number (n), core radius (r_n), and surface number density of the surfactant molecules at the interface (α_s) have also been computed. Droplet size in the case of the AOT+hexane+methanol system primarily depends on the molar ratio ω, according to $r_n=0.545(\pm0.021)+0.366(\pm0.006)\omega$. The phase behavior showing the realm of existence of microemulsion for the systems AOT+hexane+ethyleneglycol/methanol has been delineated at 30 °C. [S1063-651X(99)03504-7]

PACS number(s): 82.70.Kj

I. INTRODUCTION

In comparison to aqueous based microemulsions, there are fewer reports in the field of nonaqueous microemulsions. These are industrial systems which have been explored with regard to various aspects. Peyrelasse and co-workers [1,2] have investigated the system glycerol/sodium bis(2-ethylhexyl)sulfosuccinate (AOT)/isooctane at 25 °C and discussed the properties of this nonaqueous microemulsion in terms of a percolation phenomenon which is typical of aqueous microemulsions. Nonaqueous dispersions glycerol/AOT/ n-heptane have been studied using dynamic light scattering and viscometry by Robinson and co-workers [3]. It was found that droplet size is independent of temperature and depends primarily on the molar ratio (ω) of glycerol to AOT.

Dörfler and Borrmeister [4] have mapped the phase diagrams of nonaqueous microemulsions formed by a four component system of the nonaqueous liquid/Triton X-114/pentanol/dodecane type. The so-called water replacement components are dimethylsulphoxide, γ-butyrolactone, and acetonitrile. Recently we have investigated the ternary nonaqueous microemulsion system containing AOT+ethylbenzene+ethyleneglycol [5] over a wide range of volume fraction of dispersed phase ϕ and different molar concentration ω.

In this paper the spectrum of the nonaqueous polar components (NPC) or so-called ''water replacement components'' for the microemulsification was broadened. The NPC's chosen in the present investigation are ethyleneglycol, 2-pyrrolidinone, glycerol, and methanol. The phase diagrams of the systems AOT+hexane+ethyleneglycol and AOT+hexane+methanol were systematically investigated. Furthermore, these nonaqueous microemulsions were analyzed with respect to the influence of such systems on various volumetric and transport properties. Structural parameters such as aggregation number, i.e., the number of AOT molecules per droplet (n), core radius (r_n), and surface number density of surfactant molecule at interface (α_s) have also been calculated.

II. EXPERIMENT

The aqueous system is the starting point for the analysis of a nonaqueous system. The microemulsions were prepared by mixing appropriate amount of AOT (Fluka), hexane (E-Merck), and water or a nonaqueous polar component. The water replacement components are ethyleneglycol (Sisco Research Laboratories), 2-pyrrolidinone (Sisco Chemical Industries), glycerol (Qualigens), and methanol (E-Merck). For AOT+hexane+2-pyrrolidinone/glycerol/water systems, microemulsion formulation is possible only for $\omega=2$, whereas for AOT+hexane+methanol and AOT+hexane +ethyleneglycol systems, it varies up to 4.5 and 3, respectively. A dilution series of these microemulsions was prepared by fixing molar ratio $\omega=[NPC]/[AOT]$ but varying volume fraction in the range of $\phi\approx0-0.55$. For AOT, critical micellar concentration [6] is of the order of $10^{-3}-10^{-4}$ mol dm^{-3}, which is much lower than the concentration used in these experiments and therefore all the surfactant is considered to be localized at the interface. Assuming negligible penetration of oil phase at the interface, the ϕ is defined as volume fraction occupied by the dispersed phase (AOT+NPC) in the bulk organic phase

$$\phi=\frac{V_{AOT}+V_{NPC}}{V_{AOT}+V_{hexane}+V_{NPC}}.$$

In the determination of the phase diagram, the samples were equilibrated in a thermostated water bath maintained at 30 ± 0.1 °C. For each point in this phase diagram, the composition of the three components is summed up in wt % composition and 100% composition was obtained.

———
*Author to whom correspondence should be addressed. Electronic address: skmehta@panjabuniv.chd.nic.in
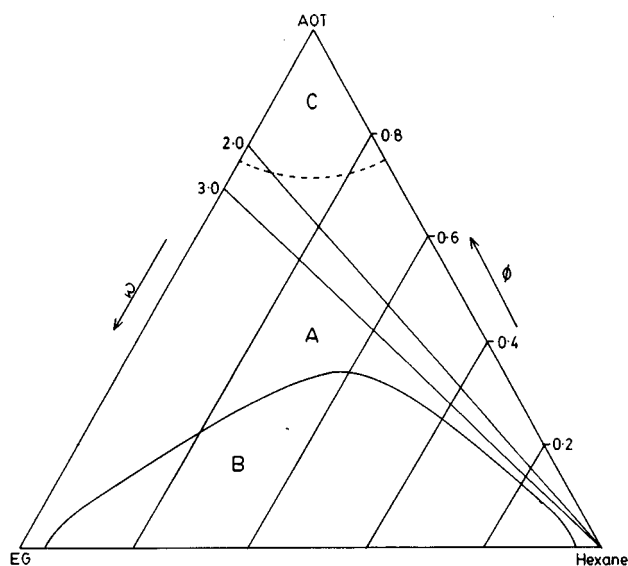
FIG. 1. Phase diagram of AOT+hexane+ethyleneglycol micro-emulsion system at 30 °C. A—single phase, B—double phase, C—mesophase.

$$X\% \ \text{AOT} + Y\% \ \text{hexane} + Z\% \ \text{NPC} = 100\%. \tag{1}$$

Phase separation took place within a few minutes but the samples were placed in a water bath for hours/days to attain the proper equilibrium. The positions of these phase boundaries were reproducible. The phase behavior of AOT +hexane+ethyleneglycol/methanol ternary microemulsion systems exhibits a single phase, double phase, and mesophase regions, which are sensitively dependent on the NPC to surfactant molar ratio, i.e., ω (Figs. 1 and 2). A large one phase region (A) exists at lower ω. The region labeled B represents the double phase. At very high concentration of emulsifier, the system is highly viscous, which is due to mesophase C. In the case of the AOT+hexane+methanol system the area under two phase region (B) has been shrunken
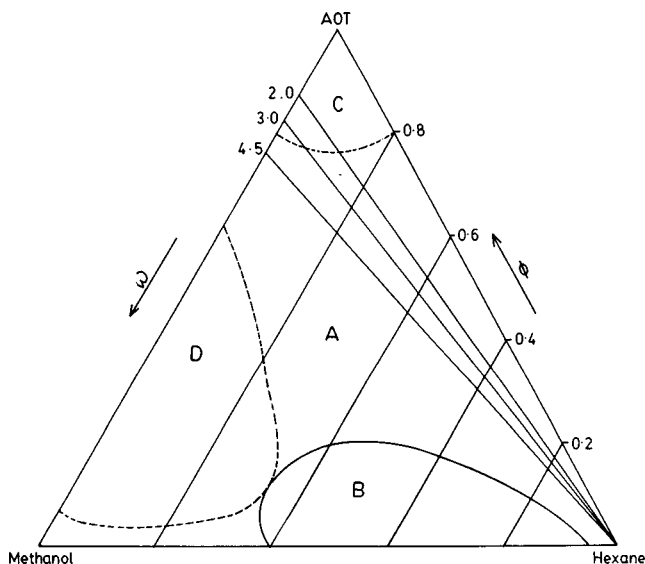

FIG. 2. Phase diagram of AOT+hexane+methanol microemulsion system at 30 °C. A—single phase, B—double phase, C—mesophase, D—suspension phase.

and shifted towards the oil rich corner. This system has an additional phase (D) showing suspended type formulations towards the methanol-AOT corner.

The conductivities of the nonaqueous microemulsions were measured in a thermostated glass cell with two platinum electrodes and digital conductivity bridge NDC 732 operating at 50 Hz from Naina Electronics. The electrodes were inserted in the double walled glass cell connected to a thermostated water bath containing microemulsion. The temperature of the sample was monitored. Sufficient time was allowed for equilibration. All measured samples were single phase and optically transparent under conditions of conductivity measurements. The cell constant of the cell used was 1.0 cm^{-1}. Measurement of conductivity was carried out with an absolute accuracy up to ±3%.

Viscosity measurements were made using a modified form of Ubbelholde's viscometer placed in a thermostated water bath. The estimated error in viscosity is less than 0.3%. The densities were measured with the help of the Anton Paar densimeter (DMA-60). The absolute uncertainty for density is estimated to be less than 10^{-5} g cm^{-3}.

An ultrasonic time intervalometer (UTI-101) from Innovative Instruments based on pulse echo overlap technique (PET) coupled with an oscilloscope was used for the precise measurements of ultrasonic velocities. The principle of measurements is to make the two signals of interest overlap on the oscilloscope by driving the X axis with frequency whose period is the travel time between the signals of interest. The frequency of sound was 2.0 MHz. The cell for the speed of sound measurements was calibrated with water as a reference. The precision in measured ultrasonic velocity values is ±0.3%.

III. RESULTS AND DISCUSSION

A. Structural parameters

We begin the analysis of nonaqueous based microemulsions by computing the structural parameters using a simple structural model. In this model, a monodisperse population of spherical droplets of disperse phase is considered to be separated from the organic phase by a monolayer of AOT. The radius of the droplets is the sum of the radius of the nonaqueous core (r_n) and the length of the surfactant tails (l). The value of ϕ allows us to calculate the core radius (r_n) and the aggregation number (n) which is the number of AOT molecules per NPC droplet. The aggregation number [7] (n) is defined as

$$n = \frac{N_{\text{AOT}}}{N_d}, \tag{2}$$

where N_{AOT} represents the total number of AOT molecules and N_d is the number of NPC droplets in total volume V_T. Therefore the above equation is written as

$$n = \frac{n_{\text{AOT}} N_A}{\phi(V_T/V_d)}, \tag{3}$$

where N_A is Avogadro's number and V_d is the total volume of the droplet (including the surfactant tail of length l), given by

$$V_d = \frac{4\pi}{3}(r_n + l)^3. \tag{4}$$

In the spherical droplet model, r_n is related to the volume fraction of droplet core V_n, as

$$r_n = \left(\frac{3}{4\pi} V_n\right)^{1/3}. \qquad (5)$$

As the number of NPC molecules per droplet is $n\omega$, Eq. (5) can be rewritten in terms of the specific volume of NPC molecules in micelles (S_n)

$$r_n = \left(\frac{3}{4\pi} S_n n\omega\right)^{1/3}. \qquad (6)$$

Thus from Eqs. (3)–(6) we get

$$n = \frac{n_{AOT}N_A}{\phi V_T}\frac{4\pi}{3}\left[\left(\frac{3}{4\pi} S_n n\omega\right)^{1/3} + l\right]^3 \qquad (7)$$

or

$$n = \frac{4\pi}{3}l^3\left[\left(\frac{\phi V_T}{n_{AOT}N_A}\right)^{1/3} - (S_n\omega)^{1/3}\right]^{-3}. \qquad (8)$$

The two unknown parameters in Eq. (8) are l and S_n. Day et al. [3] have reported the value of l for AOT as 1.03 nm. The specific volume of NPC molecules (S_n) is calculated by using molecular weight (M_{NPC}) and density of NPC (ρ_{NPC}) as ($M_{NPC}/N_A\rho_{NPC}$). Thus, the value of n and r_n can be obtained from Eqs. (8) and (6), respectively. Surface number density of surfactant molecules at interface (α_s) has been calculated using the equation

$$\alpha_s = \frac{n}{(\text{core surface area})} = \frac{n}{4\pi r_n^2}. \qquad (9)$$

At constant $\omega = 2$, with change in NPC, the value of r_n increases in the order water<methanol<ethyleneglycol <glycerol<2-pyrrolidinone.

This order may be correlated with respective molar volumes. Figure 3 represents a linear dependence of r_n with respect to molar volume (V_m) of different NPC's. Table I lists the values of n, r_n, α_s, and V_m calculated for different NPC's.

Table I shows that the systematic variation of ω has a well defined effect on the structure of the droplets in the case of the AOT+hexane+methanol system. The equation
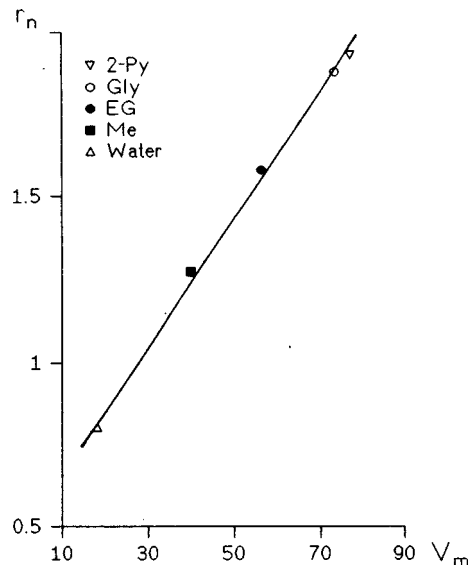

FIG. 3. Variation of core radius r_n (nm) vs molar volume V_m (cm^3 mol^{-1}) for AOT+hexane+NPC system; 2-pyrrolidinone (2-Py), ethyleneglycol (EG), methanol (Me), glycerol (Gly), water.

$$r_n = 0.545(\pm 0.021) + 0.366(\pm 0.006)\omega \qquad (10)$$

establishes a linear relationship between ω and r_n, which is in good agreement with previous measurements [5,8,9]. There is now increasing evidence [10] to suggest that the linear relationship is the result of various competing factors which conceal the underlying complexity of the structural changes.

The value of interfacial area a_{AOT} per AOT molecule may be calculated from the value of slope of the graph between ω and r_n. For a spherical microemulsion droplet containing a core of phase s (volume per molecule is equal to V_s) and containing n_{AOT} surfactant molecules having an interfacial area a_{AOT} per AOT molecule (assuming that all AOT is interfacially bound), particle surface area and particle core volume are given by

$$(\text{particle surface area}) = 4\pi r_n^2 = n_{AOT}a_{AOT}, \qquad (11)$$

$$(\text{particle core volume}) = \frac{4\pi}{3}r_n^3 = n_{AOT}\omega V_s, \qquad (12)$$

TABLE I. The value of n, r_n, α_s, V_m, and μ for the AOT+hexane+NPC microemulsion system at 30 °C.

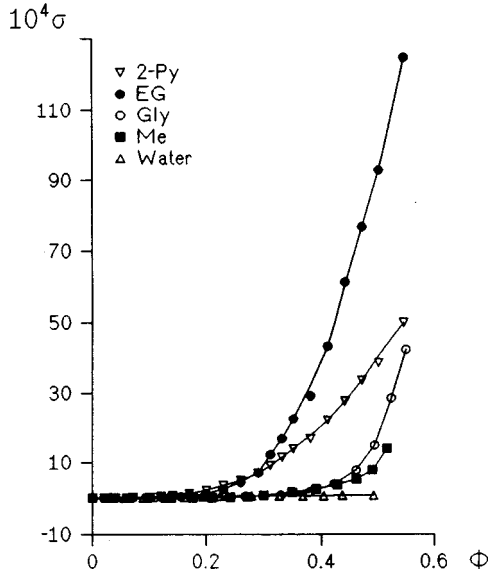| Name of NPC	ω	n	r_n (nm)	α_s (nm^{-2})	V_m (cm^3 mol^{-1})	μ (debye)
Water	2.0	36.10	0.80	4.46	18.08	1.82
Methanol	2.0	64.76	1.27	3.19	40.04	2.87
	3.0	94.72	1.65	2.76		
	4.5	146.76	2.19	2.44		
Ethyleneglycol	2.0	88.87	1.58	2.83	56.10	2.31
	3.0	135.57	2.08	2.48		
Glycerol	2.0	113.86	1.88	2.57	73.37	2.56
2-pyrrolidinone	2.0	120.37	1.93	2.57	77.16	3.55

FIG. 4. Variation of conductivity $10^4\sigma$ (S m^{-1}) vs volume fraction of dispersed phase ϕ for AOT+hexane+NPC system.

FIG. 5. Variation of conductivity $10^4\sigma$ (S m^{-1}) vs volume fraction of dispersed phase ϕ for (a) AOT+hexane+ethyleneglycol system, (b) AOT+hexane+methanol system.

where r_n represents the radius of the central droplet core. Combining Eqs. (11) and (12) yields

$$r_n = \frac{3\omega V_{NPC}}{a_{AOT}}. \tag{13}$$

V_{NPC} is the volume of a single NPC molecule. The model assumes the monodisperse collection of droplets so the slope ω vs r_n is equated with $3V_{NPC}/a_{AOT}$ to yield an apparent value of a_{AOT}. For the AOT+hexane+methanol system the value of a_{AOT} obtained is 0.547 nm^2 in comparison to the value of 0.465 nm^2 for the AOT+hexane+water system.

B. Transport properties

Figure 4 shows the variation of conductivity (σ) as a function of volume fraction of dispersed phase (ϕ) at 30 °C for AOT+hexane+NPC at $\omega=2$. The magnitude of σ increases in the order water<methanol<glycerol<ethyleneglycol <2-pyrrolidinone.

For the systems AOT+hexane+ethyleneglycol ($\omega=2,3$) and AOT+hexane+methanol ($\omega=2,3,4.5$) it is observed that by increasing ω values, the magnitude of σ increases because with increase in ω, ionic strength decreases and spontaneous radius of the surfactant increases (Fig. 5).

Electrical conductivity measurements have been used to provide information on the continuity of the aqueous phase. Like aqueous microemulsion [11–17] the present nonaqueous microemulsion also shows a percolation phenomenon in conductance. When the volume fraction of the dispersed phase is small, the interactions are so weak that the droplets may be regarded as an assembly of dynamical noninteracting isolated spheres dispersed in the continuum oil phase. But with further increase in ϕ, the attractive interactions between the droplets prolong the lifetime of the particle encounters and produce a cluster of droplets that at sufficiently high ϕ, called the critical value of the volume fraction ϕ_c, may percolate into an infinite dynamic or static interconnected net-
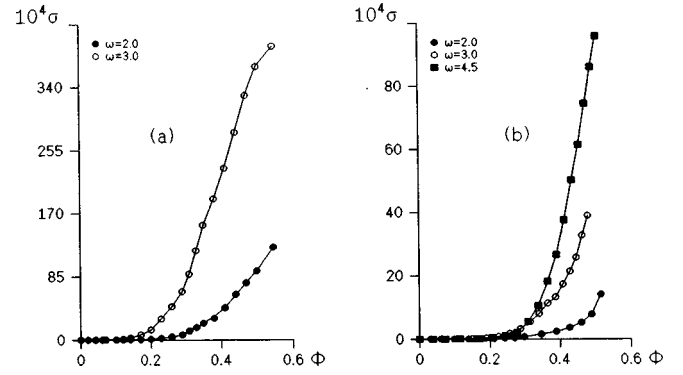
work. In the dynamic percolation model, the attractive interdroplet interactions are responsible for the percolative clusters [18–20] and the conductivity is mainly due to the efficient transfer of charge carrier between the disperse phase globules.

An alternative view for the conductivity transition in terms of the static percolation model [21] states that the conductivity transition is mainly caused by the formation of a continuous connected disperse phase in the system. Several experimental investigations together [22–24] with theoretical [18] argument provide additional support in favor of the former view, i.e., the dynamic percolation. However, the exact molecular mechanisms of the percolation are still not known.

The concept of percolation can be expressed as follows, if it is assumed that the two components are conductors with conductivity σ_1 and σ_2. For a heterogeneous system composed of these two components, the conductivity σ is given by the relation [1]

$$\sigma = \begin{cases} C_2\sigma_2(\phi_c-\phi)^{-s} & \text{where} \quad \phi<\phi_c \quad (14) \\ C_1\sigma_1(\phi-\phi_c)^t\left[1+\dfrac{C_1'\sigma_2}{C_1\sigma_1}(\phi-\phi_c)^{-(t+s)}\right] & (15) \\ \qquad\text{where} \quad \phi>\phi_c, \end{cases}$$

where C_1, C_1', and C_2 are constants and t and s are exponents which are positive.

As $(t+s)$ is positive, the σ_2/σ_1 does not tend towards infinity, while ϕ is close to ϕ_c. If $\sigma_2/\sigma_1\ll1$ (e.g., for perfect insulators $\sigma_2=0$) close to percolation threshold, we can have

$$\sigma = \begin{cases} A(\phi_c-\phi)^{-s} & \text{where} \quad \phi<\phi_c \quad (16) \\ B(\phi-\phi_c)^t & \text{where} \quad \phi_c<\phi, \quad (17) \end{cases}$$

where A and B are free parameters.

These laws are only valid near percolation threshold (ϕ_c). It is impossible to use these laws at extremely small dilutions ($\phi\to0$) or at limit concentration ($\phi\to1$) and in the immediate vicinity of ϕ_c. Previous investigations have shown that t varies from 1.2 to 2.1. Grannan, Gailand, and Tanner [25] and Song et al. [26] have suggested $s=0.7$
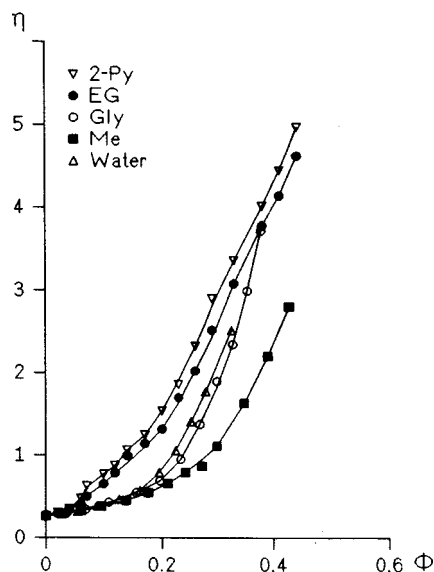
FIG. 6. Variation of viscosity η (cP) vs volume fraction of dispersed phase ϕ for the system AOT+hexane+NPC.

FIG. 7. Variation of $d(\log_{10} \eta)/d\phi$ vs volume fraction of dispersed phase ϕ for the system AOT+hexane+2-pyrrolidinone.

whereas Peyrelasse and Boned [1] have utilized $s = 1.2$ for dynamic systems of nonaqueous microemulsions.

The variation of viscosity (η) with volume fraction of dispersed phase (ϕ) has been depicted in Fig. 6. The η increases in the order methanol<glycerol<water <ethyleneglycol<2-pyrrolidinone.

For the present nonaqueous microemulsion systems, viscosity also shows a percolation phenomenon and obeys percolation laws. However, the viscosity percolation theory is far less developed than complex permittivity percolation theory. We can write the following equations for viscosity, in analogy with the equations in the case of conductance:

$$\eta = \begin{cases} C_2'' \eta_2 (\phi_c - \phi)^{-s'} & \text{if } \phi < \phi_c \quad (18) \\ C_1'' \eta_1 (\phi - \phi_c)^{t'} & \text{if } \phi > \phi_c \quad (19) \end{cases}$$

in which s' and t' are the two positive exponents, η_1 and η_2 are the viscosities of NPC and oil, respectively. Equations (18) and (19) are valid only if $\eta_2/\eta_1 \ll 1$. This condition is fully satisfied by the nonaqueous systems where the viscosity of oil (η_2) is much smaller than the viscosity of NPC (η_1).

The variation of $d(\log_{10} \eta)/d\phi$ vs ϕ shown in Fig. 7 presents a maximum which corresponds to the percolation threshold ϕ_c. The resulting ϕ_c value is close to the value obtained by the numerical estimate of the maximum of $d(\log_{10} \sigma)/d\phi$ vs ϕ (Fig. 8). Figures 9 and 10 also show good agreement between the experimental and calculated values of $\log_{10} \sigma$ vs ϕ and $\log_{10} \eta$ vs ϕ, respectively. By fitting the different values in Eqs. (16) and (17), and (18) and (19), the values of exponents s and t for dynamic conductivity and s' and t' for dynamic viscosity are obtained in the range (0.5–1.4) and (1.1–2.4), respectively.

This shows that the exponents s and s', and t and t' of dynamic conductivity and viscosity appear to be those which occur in the dynamic model of percolation of microemulsions ($s = s' = 1.2$ and $t = t' = 1.94$). This illustrates the general character of the phenomenon of dynamic percolation of microemulsions.
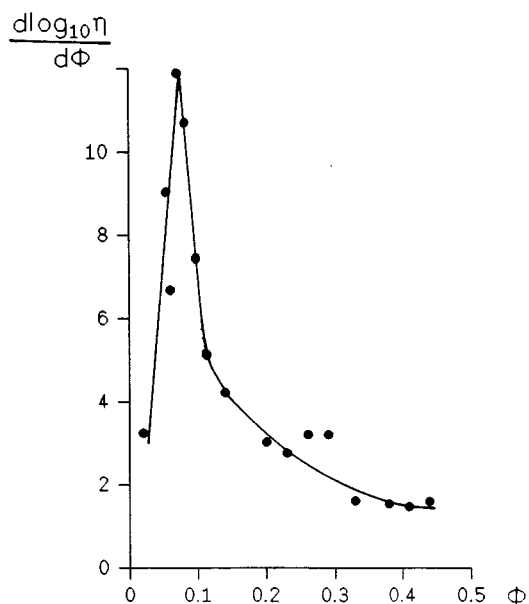
C. Charge fluctuation model

We have also calculated the specific conductance with the help of the droplet charge fluctuation model of Eicke, Borkovec, and Gupta [27]. In this model, which is valid for the freely diffusing species, it is assumed that the net charge of a droplet (which contains negative ions in the head groups of surfactant molecules and Na$^+$ counterions dispersed in the NPC pool fluctuates) around an average net zero charge and its transport is associated with the free diffusive process of single droplets. The details of the model are explained below.

Consider a nanodroplet composed of N_1 negatively charged surfactant molecules and N_2 positively charged counterions. For electroneutrality the average values are
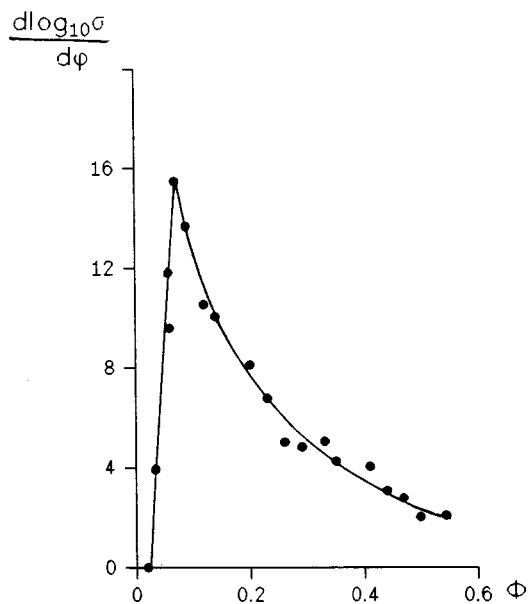

FIG. 8. Variation of $d(\log_{10} \sigma)/d\phi$ vs volume fraction of dispersed phase ϕ for the system AOT+hexane+2-pyrrolidinone.
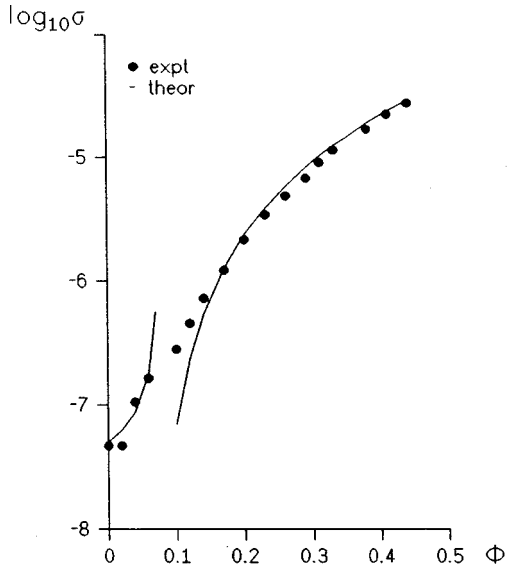
$\log_{10} \sigma$

FIG. 9. Variation of $\log_{10} \sigma$ vs volume fraction of dispersed phase ϕ for the system AOT+hexane+2-pyrrolidinone.

equal, $\langle N_1 \rangle = \langle N_2 \rangle = N$. However, due to spontaneous fluctuations in these numbers, the droplet will carry an excess charge

$$z = N_2 - N_1 \qquad (20)$$

in units of the elementary charge e. Even though the valency of a droplet z will fluctuate in time, the conductivity of a NPC in oil microemulsion and a dilute electrolyte solution containing different ions can be evaluated in an entirely equivalent manner. This is because only the mean-square valency of the ions (or droplets) determines the conductivity. The conductivity σ of a dilute electrolyte solution of different ions i with a valency z_i radius r_n (taken as independent of i for simplicity), and number density ρ_i is given by [28]

$$\sigma = \frac{e^2}{6 \pi \eta r_n} \sum_i z_i^2 \rho_i, \qquad (21)$$
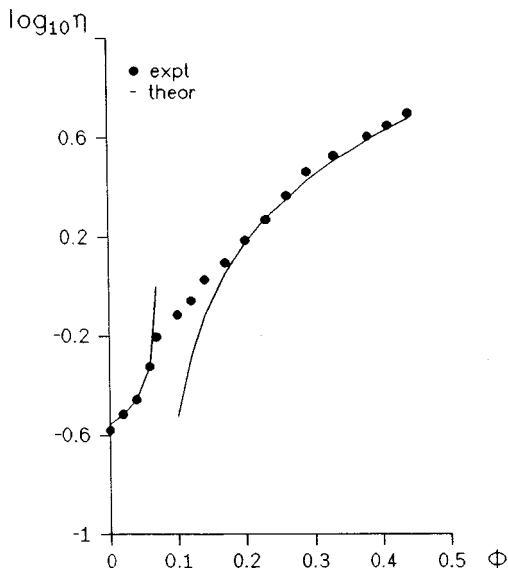
$\log_{10} \eta$

FIG. 10. Variation of $\log_{10} \eta$ vs volume fraction of dispersed phase ϕ for the system AOT+hexane+2-pyrrolidinone.

where η is the viscosity of the solvent and i runs over all different ionic species in the solution. In the case of microemulsion droplets it is more convenient to write Eq. (21) as

$$\sigma = \frac{\rho e^2}{6 \pi \eta r_n} \langle z^2 \rangle, \qquad (22)$$

where ρ is the number of droplets per unit volume and $\langle \ \rangle$ is the canonical average over all droplets. Note that due to electroneutrality $\langle z \rangle = 0$.

The quantity of interest is the mean-square charge $\langle z^2 \rangle$ of a droplet. It can be expressed in terms of the mean-squared fluctuations of the number of ions residing on a droplet $\delta N_i = N_i - \langle N_i \rangle$ by

$$\langle z^2 \rangle = \langle \delta N_2^2 \rangle - 2 \langle \delta N_2 \delta N_1 \rangle + \langle \delta N_1^2 \rangle. \qquad (23)$$

Such averages are related to derivatives with respect to the conjugated thermodynamic forces [29]

$$\langle \delta N_i \delta N_j \rangle = k_B T \left(\frac{\partial N_i}{\partial \mu_j} \right)_{T, \mu_{k \neq j}}, \qquad (24)$$

where μ_j is the chemical potential of the jth component ($j = 1,2$), T is the absolute temperature, and k_B is the Boltzmann constant.

To evaluate $\langle z^2 \rangle$ explicitly, one needs a model for the chemical potential μ_i of the ion residing on a droplet. One may write

$$\mu_i = \mu_i^{(0)} + k_B T \ln N_i + \mu_i^{(ex)}, \qquad (25)$$

where the first two terms on the right-hand side represent the chemical potential for an ideal solution while $\mu_i^{(ex)}$ is the excess chemical potential

$$\mu_i^{(ex)} = \left(\frac{\partial G^{(ex)}}{\partial N_i} \right)_{T, N_{k \neq j}}. \qquad (26)$$

We adopt a very simple model and identify the electrostatic work required to charge a droplet in the solvent with the excess Gibbs free energy, i.e.,

$$G^{(ex)} = \frac{z^2 e^2}{8 \pi \varepsilon_0 \varepsilon r_n}, \qquad (27)$$

where z is given in Eq. (20), ε_0 is the dielectric permittivity of the vacuum, and ε is the dielectric constant of the solvent. The excess Gibbs free energy [Eq. (27)] is also the basis of Born's theory of ionic solvation.

Now we will calculate $\langle z^2 \rangle$ explicitly. Using Eqs. (25)–(27), the 2×2 matrix with the elements $(\partial \mu_i / \partial N_j)_{N_{k \neq j}, T}$ was evaluated and it was found that

$$k_B T \begin{bmatrix} 1/N_1 + \alpha & -\alpha \\ -\alpha & 1/N_2 + \alpha \end{bmatrix}. \qquad (28)$$

The abbreviation $\alpha = e^2/(4 \pi k_B T \varepsilon_0 \varepsilon r_n)$ has been introduced. The derivatives $(\partial N_i / \partial \mu_j)_{\mu_{k \neq j}, T}$ required in Eq. (24) can be obtained most easily by noting the fact that the matrices with the elements $(\partial \mu_i / \partial N_j)_{N_{k \neq j}, T}$ and

TABLE II. Experimental and calculated specific conductances in the low ϕ region of AOT+hexane+NPC microemulsions at 30 °C.

Name of NPC	ω	$\phi - \phi_c$	$\left(\dfrac{\sigma}{\phi}\right)_{expt}$ (units of 10^4)	$\left(\dfrac{\sigma}{\phi}\right)_{theor}$ (units of 10^4)
Water	2.0	0.028–0.194	1.25–1.80	7.29
Methanol	2.0	0.031–0.299	1.51–2.39	1.83
	3.0	0.033–0.147	0.30–0.88	0.84
	4.5	0.037–0.162	0.27–0.74	0.36
Ethyleneglycol	2.0	0.038–0.074	1.52–1.89	0.95
	3.0	0.038–0.120	10.20–13.06	0.42
Glycerol	2.0	0.036–0.268	1.63–1.92	0.57
2-pyrrolidinone	2.0	0.038–0.070	2.73–3.15	0.52

$(\partial N_i / \partial \mu_j)_{\mu_{k \neq j}, T}$ are related by simple matrix inversion [29]. Inverting the matrix in Eq. (28) and using Eqs. (24) and (23), it gives

$$\langle z^2 \rangle = \frac{2N}{1 + 2N\alpha}. \tag{29}$$

There are two limiting cases to consider. For $\alpha \ll 1$ the second term in the denominator of Eq. (29) is negligible, and therefore $\langle z^2 \rangle = 2N$. This is the limiting case of ideal behavior where the mean-square fluctuations are essentially given by the number of ions residing on the droplet. As $N \gg 1$, the realistic case corresponds to the second limit where $\langle z^2 \rangle = 1/\alpha$. This means that it is determined by the ratio of Coulomb and thermal energies. Inserting $\langle z^2 \rangle = 1/\alpha$ into Eq. (22), we obtain the final result for the conductivity of a dilute microemulsion

$$\sigma = \frac{\varepsilon_0 \varepsilon k_B T}{2 \pi \eta} \frac{\phi}{r_n^3}. \tag{30}$$

ρ has been replaced with the volume fraction of the droplets ϕ by using the relation $\phi = 4 \pi r_n^3 \rho / 3$. Equation (30) predicts that the specific conductivity in a NPC in oil microemulsion σ / ϕ should be constant and, for a given solvent and temperature, depend on the radius of the droplets only ($\propto r_n^{-3}$). This result is independent of the charge of the ions in question. As seen from Table II, the comparison of the $(\sigma / \phi)_{calc}$ and $(\sigma / \phi)_{expt}$ data (maximum and minimum values in the low ϕ region) shows a satisfactory agreement between the two and they are of the same order of magnitude. The observed deviations occurred due to low values of ω, where droplets are smaller in size. Such a result has been noticed by Eicke, Borkovec, and Gupta [27] in isooctane and by Aprano [30] in n-heptane microemulsions. The values of r_n required for the above calculations were evaluated from Eq. (6). The ε and η used for hexane are 1.8799 and 0.2942 [31], respectively.

D. Volumetric properties

Ultrasonic has proved to be a useful tool for acquiring information about the dynamics of liquid systems. The mea-

surement of ultrasonic velocity enables the accurate determination of isentropic compressibility k_s, a more sensitive parameter to structural changes. The interfacial region of a droplet should show different compressibility characteristics relative to that of the remaining portion of the microphase droplets because of the chemical and electrical gradients that can occur across the interfacial region, particularly when amphiphile species are located at the surface. The isentropic compressibility (k_s) was calculated from u and ρ for the microemulsion using the relation

$$k_s = 1/u^2 \rho, \tag{31}$$

which assumes that dissipative effects are negligible and that the hydrodynamic equation of motion can be linearized.

The densities of these nonaqueous microemulsions for $\omega = 2$ at 30 °C show a linear trend. With increase in ϕ, ρ increases in the order water<methanol<glycerol <ethyleneglycol<2-pyrrolidinone.

A plot between u and ϕ at constant T (Fig. 11) shows a decrease in u with increasing ϕ and then a sharp increase in u. There is no evidence of discontinuity in ultrasonic velocity
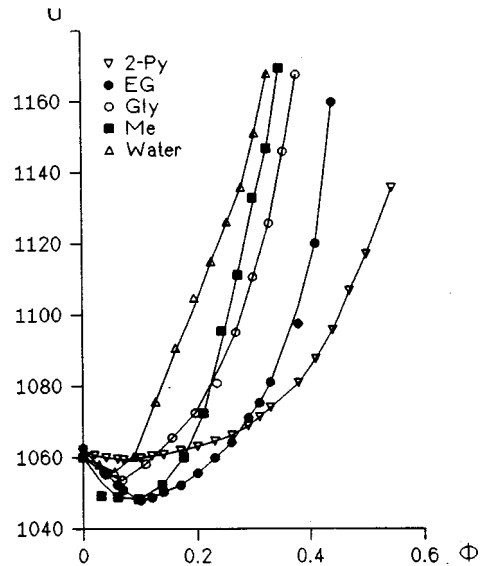

FIG. 11. Variation of ultrasonic velocity u (m s^{-1}) vs volume fraction of dispersed phase ϕ for the system AOT+hexane+NPC.
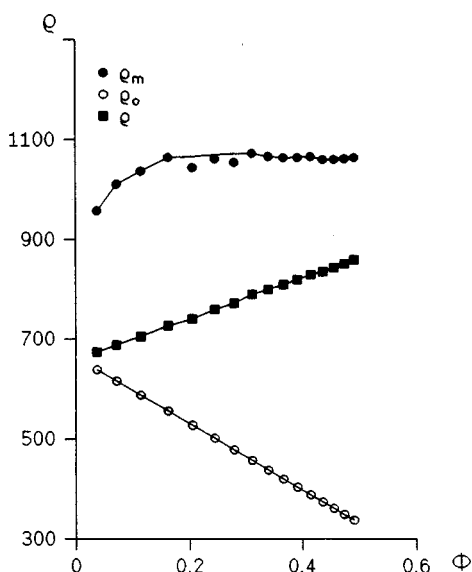
FIG. 12. Variation of density ρ (kg m^{-3}) vs volume fraction of dispersed phase ϕ for the system AOT+hexane+methanol ($\omega=4.5$).
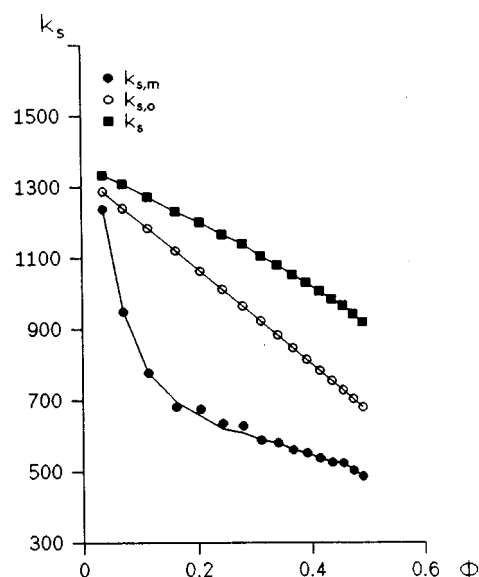

FIG. 13. Variation of isentropic compressibility k_s (TPa^{-1}) vs volume fraction of dispersed phase ϕ for the system AOT+hexane+methanol ($\omega=4.5$).

over the entire range. With increase in ϕ, u increases in the order 2-pyrrolidinone<ethyleneglycol<glycerol<methanol <water.

As from literature, it may also be considered that the microemulsions are made up of two noninteracting regions, the micellar phase containing drops and bulk phase or oil phase in w/o microemulsions [30–32]. Assuming the volume additions of micellar phase and bulk phase, the total density and isentropic compressibility of the system is given by the relation

$$\rho = \phi_m \rho_m + (1 - \phi_m)\rho_o, \qquad (32)$$

$$k_s = \phi_m k_{s,m} + (1 - \phi_m)k_{s,o}, \qquad (33)$$

where ϕ_m and ϕ_o are the volume fractions of the micellar and oil phase, respectively. ρ_m and $k_{s,m}$ are the micellar density and isentropic compressibility of micellar phase whereas ρ_o and $k_{s,o}$ are the density and isentropic compressibility of the oil phase. ρ_m and $k_{s,m}$ calculated from the above relations are plotted against ϕ in Figs. 12 and 13, respectively. It is concluded that with increase in ϕ, ρ_m shows a little increase at low ϕ and then becomes constant whereas $k_{s,m}$ decreases at low ϕ and becomes almost constant at higher ϕ. The variation in ρ_m and $k_{s,m}$ is not very prominent, showing that the size of the particle is not dependent on ϕ.

IV. CONCLUSIONS

In all the systems, the conductivity and viscosity increase with increase in ϕ. Both the properties exhibit the percolation phenomenon. By fitting different values in scaling laws, the calculated values of $s=s'$ and $t=t'$ are in the range 0.5–1.4 and 1.1–2.4, respectively. The conductivity is explained by the migration of charged droplets in the electric field. A satisfactory agreement between $(\sigma/\phi)_{\text{expt}}$ and

$(\sigma/\phi)_{\text{calc}}$, calculated from the prediction of the charge fluctuation model, has been observed. These charged droplets are formed by spontaneous number fluctuations of the ions residing on the droplets. The magnitude of these fluctuations is directly related to the Coulomb energy that is required to charge up a droplet. Density shows a linear trend with ϕ whereas ultrasonic velocity first decreases and then starts increasing. The calculated ρ_m value decreases and $k_{s,m}$ value increases with ϕ but the change is not very prominent, showing that the size of the particle is not dependent on ϕ. For a particular ω, the core radius (r_n) remains constant at different values of ϕ but it varies linearly with respect to ω. The interfacial area occupied by AOT molecules in a nonaqueous system (AOT+hexane+methanol) is 0.547 nm^2 as compared to 0.465 nm^2 of the aqueous AOT+hexane+water system. In the phase diagram of AOT+hexane+ethyleneglycol/methanol systems, ternary nonaqueous microemulsions are formed towards the oil rich corner at lower ω.

It can be concluded that replacing water by methanol, glycerol, ethyleneglycol, and 2-pyrrolidinone, microemulsions are formed. These nonaqueous microemulsions are formed as spontaneously as in the aqueous system. However, the polar components bring about some changes in the hydrogen bonding equilibria and electrostatic interactions in the microemulsification. The NPC's have more enhanced molecular interaction with the hydrophobic compounds than water (cf. $\mu_{\text{NPC}} > \mu_{\text{H}_2\text{O}}$). This difference leads to higher penetration of NPC molecules in the hydrocarbon part of the surfactant. The high penetration means an increase in cross sectional area of the surfactant, i.e., AOT is more closely packed at the NPC interface. The effect will be more pronounced with 2-pyrrolidinone because of its cyclic structure and better hydrogen bonding capability whereas among the other three it varies as bonding sites decrease, i.e., glycerol($\varepsilon=42.5$)>ethyleneglycol($\varepsilon=37.7$) >methanol($\varepsilon=32.7$).

[1] J. Peyrelasse and C. Boned, Phys. Rev. A **41**, 938 (1990).

[2] Z. Saidi, C. Mathew, J. Peyrelasse, and C. Boned, Phys. Rev. A **42**, 872 (1990).

[3] R. A. Day, B. H. Robinson, J. H. R. Clarke, and J. V. Doherty, J. Chem. Soc., Faraday Trans. 1 **75**, 132 (1979).

[4] H. D. Dörfler and E. Borrmeister, Tenside Deterg. **29**, 154 (1992).

[5] S. K. Mehta, Kawaljit, and Kiran Bala, Langmuir (to be published).

[6] J. Peyrelasse and C. Boned, J. Phys. Chem. **89**, 370 (1985).

[7] J. Casado, C. Izquierdo, S. Fuentes, and M. L. Moyá, J. Chem. Educ. **71**, 446 (1994).

[8] P. D. I. Fletcher, M. F. Galal, and B. H. Robinson, J. Chem. Soc., Faraday Trans. 1 **80**, 3307 (1984).

[9] B. H. Robinson, C. Toprakcioglu, J. C. Dore, and P. Chieux, J. Chem. Soc., Faraday Trans. 1 **80**, 13 (1984).

[10] P. D. I. Fletcher, A. M. Howe, N. M. Perrins, B. H. Robinson, C. Toprakcioglu, and J. C. Dore, in *Proceedings of the 3rd International Symposium, Surfactants in Solution*, edited by K. Mittal (Plenum, New York, 1983).

[11] S. K. Mehta, R. K. Dewan, and Kiran Bala, Phys. Rev. E **50**, 4759 (1994).

[12] M. Moha-Ouchane, J. Peyrelasse, and C. Boned, Phys. Rev. A **35**, 3027 (1987).

[13] S. K. Mehta and Kiran Bala, Phys. Rev. E **51**, 5732 (1995).

[14] P. Alexandridis, J. F. Holzwarth, and T. Alan Hatton, J. Phys. Chem. **99**, 8222 (1995).

[15] H. Mays, J. Phys. Chem. B **101**, 10 271 (1997).

[16] F. Caboi, G. Capuzzi, P. Baglioni, and M. Monduzzi, J. Phys. Chem. B **101**, 10 205 (1997).

[17] F. Bordi, C. Cametti, P. Codastefano, F. Sciortino, P. Tartaglia, and J. Rouch, Prog. Colloid Polym. Sci. **100**, 170 (1996).

[18] G. S. Grest, I. Webman, S. A. Safran, and A. L. R. Bug, Phys. Rev. A **33**, 2842 (1986).

[19] H. F. Eicke, R. Hilfiker, and H. Thomas, Chem. Phys. Lett. **125**, 295 (1986).

[20] S. A. Safran, I. Webman, and G. S. Grest, Phys. Rev. A **32**, 506 (1985); A. L. R. Bug, S. A. Safran, G. S. Grest, and I. Webman, Phys. Rev. Lett. **55**, 1896 (1985).

[21] P. G. de Gennes and C. Taupin, J. Phys. Chem. **86**, 2294 (1982); Y. Talmon and S. Prager, J. Chem. Phys. **69**, 2984 (1978).

[22] S. Bhattacharya, J. P. Stokes, M. W. Kim, and J. S. Huang, Phys. Rev. Lett. **55**, 1884 (1985).

[23] M. A. Van Dijk, Phys. Rev. Lett. **55**, 1003 (1985).

[24] M. W. Kim and J. S. Huang, Phys. Rev. A **34**, 719 (1986).

[25] D. M. Grannan, J. C. Gailand, and D. B. Tanner, Phys. Rev. Lett. **46**, 375 (1981).

[26] Y. Song, T. W. Noh, S. I. Lee, and J. R. Gainis, Phys. Rev. B **33**, 904 (1986).

[27] H. F. Eicke, M. Borkovec, and B. D. Gupta, J. Phys. Chem. **93**, 314 (1989).

[28] R. S. Berry, S. A. Rice, and J. Ross, *Physical Chemistry* (Wiley, New York, 1980).

[29] H. B. Callen, *Thermodynamics* (Wiley, New York, 1960).

[30] A. D'Aprano, G. D'Arrigo, A. Paparelli, M. Goffredi, and V. T. Liveri, J. Phys. Chem. **97**, 3614 (1993).

[31] J. A. Riddick and W. B. Bunger, *Organic Solvents: Physical Properties and Methods of Purification*, 3rd ed. (Wiley Interscience, New York, 1970).

[32] G. D'Arrigo, A. Paparelli, A. D'Aprano, I. D. Donato, M. Goffredi, and V. T. Liveri, J. Phys. Chem. **93**, 8367 (1989).